Profiling of Naquotinib, a Small Molecule Kinase Inhibitor, as EGFR and BTK Inhibitor

January 2022

Hiroaki TANAKA

Profiling of Naquotinib, a Small Molecule Kinase Inhibitor, as EGFR and BTK Inhibitor

A Dissertation Submitted to
the Graduate School of Science and Technology,
University of Tsukuba
in Partial Fulfillment of Requirements
for the Degree of Doctor of Philosophy in Science

Doctoral Program in Biology,
Degree Programs in Life and Earth Sciences

Hiroaki TANAKA

Table of Contents

Abbreviation

ABC DLBCL	activated B-cell-like DLBCL
AKT	protein kinase B
BCR	B-cell receptor
BMX	bone marrow kinase on the X chromosome
BTK	Bruton's tyrosine kinase
CLL	chronic lymphocytic leukemia
del ex19	deletion in exon 19
DLBCL	Diffuse large B-cell lymphoma
EGFR	epidermal growth factor receptor
ERK	extracellular signal-regulated kinase
GCB DLBCL	germinal center B-cell-like DLBCL
HRP	horseradish peroxidase
IS	internal standard
L858R	leucine-to-arginine substitution at amino acid position 858
LC-MS/MS	liquid chromatography-tandem mass spectrometry
MCL	mantle cell lymphoma
NHL	non-Hodgkin lymphoma
NSCLC	non–small cell lung cancer
pAKT	phosphorylated AKT
pBTK	phosphorylated BTK
PDX	patient-derived xenograft
pEGFR	phosphorylated EGFR
pERK	phosphorylated ERK
RLK	resting lymphocyte kinase
SEM	standard error of the mean
TBS	Tris-Buffered Saline
T790M	threonine-to-methionine substitution at amino acid position 790
TBST	TBS with Tween 20
TKI	tyrosine kinase inhibitor
TXK	resting lymphocyte kinase
WT	wild-type

General Abstract

Naquotinib is an irreversible tyrosine kinase inhibitor (TKI) originally designed to target the epidermal growth factor receptor (EGFR). A comprehensive kinase panel evaluation indicated that naquotinib inhibits Bruton's tyrosine kinase (BTK) as well as EGFR with threonine-to-methionine substitution at amino acid position 790 (T790M) resistant mutation. In order to characterize the profile of naquotinib as EGFR inhibitor and BTK inhibitor, I examined inhibitory effect of naquotinib using molecular biological, pharmacological and pharmacokinetic methods. *In vitro*, naquotinib inhibited EGFR T790M resistant kinase activity and BTK kinase activity with similar potency. In addition, naquotinib inhibited non–small cell lung cancer (NSCLC) cell lines harboring mutant EGFR and B-cell lymphoma cell lines depending on chronically active B-cell receptor (BCR) signaling. *In vivo*, naquotinib showed robust inhibition of tumor growth both in NSCLC cell lines with EGFR mutations and activated B-cell-like Diffuse large B-cell lymphoma (ABC DLBCL) cell lines. Pharmacokinetic studies showed that naquotinib has higher concentrations and longer half-life in tumors than plasma in NSCLC and ABC DLBCL cell line xenograft models. These findings suggest that when the inhibitor demonstrates an inhibitory activity comparable to that of the target enzyme, it has comparable cell proliferation inhibitory activity, antitumor activity, and biodistribution.

In addition, I considered the enzyme selectivity of this irreversible TKI. Although irreversible inhibition exerts strong inhibitory effect to the target, it raised concern that side effects would be strong and persistent. However, naquotinib did not affect body weight in *in vivo* xenograft models and did not show noteworthy side effects in phase I–II clinical trials. Naquotinib inhibited only a few enzymes other than EGFR and BTK, but none of them were widely known to cause side effects. In addition, naquotinib inhibited EGFR and BTK in a very similar manner. I thought that the positional relationship between the gatekeeper amino acid and the cysteine residue, to which naquotinib bonds covalently, is important for inhibition activity. *In silico* structural analysis revealed that ten kinases, including EGFR and BTK, were predicted to possess a cysteine at the same position as EGFR. Surprisingly, naquotinib did not show strong inhibitory activity against enzymes other than these 10 enzymes. In other words, naquotinib acquired superior kinase selectivity for all kinases except for such special kinases.

In this study, I have shown that increasing enzyme selectivity can create powerful yet safe covalent enzyme inhibitors. This opens the way for the creation of inhibitors not only for resistant mutant enzymes but also for targets that could not be inhibited by competitive inhibitors, such as having no definite pocket structure.

General Introduction

Cancer is defined, in a broad sense, as a mass formed by the disorderly growth of abnormal cells, and in a narrow sense, it is defined as a mass that damages normal cells, especially with infiltration and metastasis. It is known that the disorderly growth of cancer is based on the abnormal increase of growth signals triggered by the increase of growth factors and their receptors, and the abnormal activation of receptors and their downstream molecules. Kinases, activating in cancer-specifically, are good drug targets because growth signals are relayed primarily by phosphorylation of downstream molecules by kinases (1). In fact, kinase inhibitors have provided effective clinical therapies for cancer patients. This has led to the development of more kinase inhibitors since the early 2000s (2). However, as evidenced by the development of second- and third- generation kinase inhibitors, the benefits of resistance are limited.

Epidermal growth factor receptor (EGFR) mutations are detected in approximately 10% of non–small cell lung cancer (NSCLC) in Caucasian patients and approximately 40% of NSCLC in East Asian patients (3–5). Erlotinib and gefitinib have been developed as EGFR inhibitors. These drugs dramatically improve progression-free survival in patients with advanced NSCLC. However, almost all patients develop resistance to these drugs (6–9). The EGFR threonine-to-methionine substitution at amino acid position 790 (T790M) mutation of EGFR is the most predominant mechanism for resistance (10–13). This mutation alters the three-dimensional structure of the enzyme pocket, leading to decreased binding of EGFR inhibitors and increased affinity for ATP (10, 14). There was no effective drug for recurrent cancer due to the acquisition of both mechanisms, so we, I and project team members, focused on the EGFR T790M resistant mutant enzymes and started to create this resistant mutant kinase inhibitor.

First, we will clarify the profile required for resistant mutant kinase inhibitor based on the knowledge of existing EGFR inhibitors.

First-generation EGFR inhibitors are ATP-competitive reversible inhibitors such as erlotinib and gefitinib. These drugs strongly inhibit EGFR-activating mutant enzymes and weakly inhibit wild-type (WT) EGFR enzymes. Although administration of excessive doses of these agents causes side effects associated with WT EGFR enzyme inhibition, these are still used as a first-line drug for patients with EGFR-activating mutation-positive patients. On the other hand, it does not have inhibitory activity against resistant mutant enzymes.

Second-generation EGFR inhibitors, such as afatinib and dacomitinib, were developed in an attempt to overcome resistance mutations. In order to inhibit resistant mutant enzymes with enhanced affinity for ATP, covalent inhibitors that inhibit ATP non-competitively have been selected. However, structures of these drugs are not favorable for resistant mutant enzymes. In fact, it inhibited WT EGFR enzymes even more strongly than resistant mutant enzymes. On the other hand, covalent inhibitors irreversibly inhibit

the target. This characteristic raised concern that side effects would be strong and persistent. As expected, side effects due to WT EGFR enzyme inhibition, including diarrhea and painful skin disorders called rash, were strongly observed. Due to these side effects, the dose of the second-generation EGFR inhibitors could not be increased enough, and no therapeutic effect was observed in patients with resistant mutations (15–20).

Based on these findings, the profile required for EGFR T790M resistant mutant enzyme inhibitors could be determined as follows: inhibitors with a strong inhibitory activity against resistant mutant enzymes, and inhibitors with a sufficient margin for side effects from inhibiting other enzymes, including WT EGFR enzymes.

We have established the following policy to acquire such inhibitors. In order to inhibit resistant mutant enzymes strongly, we selected the covalent inhibitors following the second-generation EGFR inhibitors. In order to obtain a sufficient margin for resistant mutant enzymes to WT EGFR enzymes, we referred to the following findings. That is, compounds that bind to an inactive state EGFR enzyme, such as neratinib, inhibit WT EGFR enzymes and EGFR-activating mutant enzymes with the comparable activity, while compounds that bind to an active state EGFR enzyme, such as gefitinib, inhibit EGFR-activating mutant enzymes rather than WT EGFR enzymes (15). Therefore, we aimed at inhibitors that bind to active state EGFR enzyme. We also aimed at compounds that have an affinity for EGFR T790M resistant mutant-specific amino acid, the methionine substituted for threonine at amino acid position 790.

We have established the following plans for the screening and optimization research process. We constantly evaluated the inhibitory activity against resistant mutant enzymes and WT enzymes. In addition, we appropriately performed co-crystal structure analysis and *in silico* structure analysis of resistant mutant enzymes and compounds. Furthermore, we conducted a comprehensive kinase panel evaluation and confirmed the selectivity of enzymes other than EGFR. For *in vivo* evaluation, we have examined the antitumor effect using a xenograft model. Finally, we found naquotinib, T790M resistant mutant-selective irreversible EGFR inhibitor.

In this study, in order to characterize the profile of naquotinib as an EGFR inhibitor for patients with NSCLC with EGFR-activating mutations and T790M resistant mutation, I examined inhibitory effect of naquotinib using *in vitro* enzyme inhibition assays, *in vitro* cell proliferation assays, immunoblotting analysis, *in vivo* xenograft studies, and pharmacokinetic studies (Chapter I).

In vitro enzyme inhibition assays revealed that naquotinib inhibits several enzymes as well as EGFR T790M resistant enzymes, including Bruton's tyrosine kinase (BTK) (21). BTK is activated in activated B-cell-like Diffuse large B-cell lymphoma (ABC DLBCL) (22). The ABC DLBCL is associated with worse prognosis using currently available therapies such as combination treatment with rituximab plus standard cytotoxic chemotherapy (23, 24). Therefore, in order to characterize the profile of naquotinib as a BTK inhibitor for the treatment of ABC DLBCL, I examined inhibitory effect of

naquotinib like as an EGFR inhibitor (Chapter II).

Here, I describe the preclinical *in vitro* and *in vivo* characteristics of naquotinib, which has a selective inhibitory effect on EGFR-activating mutations and T790M resistance mutation over WT as an EGFR inhibitor. In addition, I show the inhibitory effect of naquotinib on BTK. Furthermore, I consider the enzyme selectivity of this irreversible TKI and the contribution it makes.

Chapter I: Profiling of Naquotinib, a Small Molecule Kinase Inhibitor, as EGFR Inhibitor

Abstract

First- and second-generation epidermal growth factor receptor (EGFR) tyrosine kinase inhibitors (TKI) are effective clinical therapies for patients with non–small cell lung cancer (NSCLC) harboring EGFR-activating mutations. However, almost all patients develop resistance to these drugs. The EGFR threonine-to-methionine substitution at amino acid position 790 (T790M) mutation of EGFR is the most predominant mechanism for resistance. Here, I report that naquotinib, a pyrazine carboxamide–based EGFR-TKI, inhibited EGFR with activating mutations, as well as T790M resistance mutation while sparing wild-type (WT) EGFR. In *in vivo* murine xenograft models using cell lines and a patient-derived xenograft model, naquotinib induced tumor regression of NSCLC with EGFR-activating mutations with or without T790M resistance mutation, whereas it did not significantly inhibit WT EGFR signaling in skin. These findings suggest that naquotinib has therapeutic potential in patients with NSCLC with EGFR-activating mutations and T790M resistance mutation.

Introduction

Epidermal growth factor receptor (EGFR) mutations are detected in approximately 10% of non–small cell lung cancer (NSCLC) in Caucasian patients and approximately 40% of NSCLC in East Asian patients (3–5). EGFR mutations lead to constitutive activation of EGFR signaling, including the mitogen-activated protein kinase/extracellular signal-regulated kinase (ERK) and phosphoinositide 3-kinase/protein kinase B (AKT) pathways (25, 26) and oncogenic transformation, such as increased malignant cell survival, proliferation, invasion, metastatic spread, and tumor angiogenesis in NSCLC (27, 28). The most common EGFR mutations are deletion in exon 19 (del ex19) and leucine-to-arginine substitution at amino acid position 858 (L858R) in exon 21 mutations, which together account for approximately 90% of activating EGFR mutations in NSCLC (29, 30).

The first-generation reversible EGFR tyrosine kinase inhibitors (TKI), gefitinib and erlotinib, and second-generation covalent EGFR-TKIs, afatinib and dacomitinib, dramatically improve progression-free survival in patients with advanced NSCLC. However, almost all patients eventually develop resistance to these drugs after a median of 10–13 months (6–9). The EGFR threonine-to-methionine substitution at amino acid position 790 (T790M) mutation is the most predominant mechanism for acquired resistance, detected in approximately 50%– 60% of patients with clinical resistance to these EGFR-TKIs (10–13).

Several third-generation irreversible EGFR-TKIs, including WZ4002, osimertinib, rociletinib, and olmutinib, have been developed to target activating EGFR mutations, as well as T790M mutation while sparing wild-type (WT) EGFR because second-generation EGFR-TKIs cause dose-limiting epithelial toxicities due to their activity against WT EGFR and the normal physiologic role of this kinase in skin and gastrointestinal tissues (15–20). Although osimertinib has been approved for second-line treatment in patients with NSCLC with EGFR T790M mutation, this therapeutic option is limited.

Here, I describe the preclinical *in vitro* and *in vivo* characteristics of naquotinib, which has a selective inhibitory effect on EGFR-activating mutations and T790M resistance mutation over WT.

Materials and Methods

Reagents

Naquotinib and erlotinib were prepared at Astellas Pharma Inc. as described in PCT Patent Application WO 2016/121777 and WO2001/34574, respectively. Afatinib and osimertinib were synthesized according to the PCT Patent Application WO 2002/50043 and WO 2013/014448, respectively.

Cell lines and cell culture

NCI-H1975, HCC827, NCI-H292, and NCI-H1666 were obtained from American Type Culture Collection (ATCC, Manassas, VA, USA) in 2012, 2012, 2008, and 2008, respectively. PC-9 was obtained from Immuno-Biological Laboratories in 2011. Both II-18 and A431 were obtained from RIKEN BRC Cell Bank in 2013. Cells were cultured in RPMI1640 medium supplemented with 10% heat-inactivated fetal bovine serum at 37°C in 5% CO_2 atmosphere. The cell lines used in this study were not authenticated in our laboratory but were purchased from the providers of authenticated cell lines and stored at early passages in a central cell bank at Astellas Pharma Inc., with Mycoplasma testing performed using PCR. The experiments were conducted using low-passage cultures of these stocks.

In vitro cell proliferation assays

Human cell lines were plated the day before treatment with test reagents in 96-well white plates, in 96-well collagen type I-coated plates (AGC Techno Glass Co., LTD., Shizuoka, Japan) or in Prime Surface 96-well plates (Sumitomo Bakelite Co., Ltd., Tokyo, Japan). NCI-H1975, HCC827, PC-9 and II-18 cells were plated at 1.0×10^3 cells/well. Naquotinib was added to achieve final concentrations of 0.3, 1, 3, 10, 30, 100, 300, 1000, and 3000 nmol/L. NCI-H1975, HCC827 and II-18 cells were incubated for 4 days and PC-9 cells for 5 days. A431 and NCI-H292 cells were plated at 1.0×10^3 cells/well and NCI-H1666 cells were plated at 2.0×10^3 cells/well. Naquotinib was added to achieve final concentrations of 1, 3, 10, 30, 100, 300, 1000, 3000, and 10000 nmol/L. A431 cells were incubated for 4 days, NCI-H292 cells for 5 days and NCI-H1666 cells for 7 days.

After treatment, the CellTiter-Glo® Luminescent Cell Viability Assay (Promega) was used according to the manufacturer's instructions and luminescence was measured using an ARVO plate reader (Perkin Elmer Inc., Waltham, MA). The assay was performed in triplicate. The effect of naquotinib on cell proliferation was analyzed using SAS software (SAS Institute Inc) or GraphPad Prism (GraphPad Software). The IC_{50} value of each experiment was calculated using Sigmoid-Emax model non-linear regression analysis and was expressed as the geometric mean of three independent experiments.

Immunoblotting analysis

Protein was extracted using Cell Lysis Buffer (Cell Signaling Technology, CST, Danvers, MA, USA) or RIPA Buffer (Thermo Fisher Scientific, Waltham, MA, USA) supplemented with a Phosphatase Inhibitor Cocktail (Thermo Fisher Scientific) and Protease Inhibitor Cocktail (Sigma-Aldrich, St. Louis, MO, USA or Nacalai Tesque, Kyoto, Japan). Protein concentrations of the lysates were determined using a BCA protein assay reagent kit or Pierce 660 nm Protein Assay Kit (Thermo Fisher Scientific). Equal amounts of total protein were resolved by SDS-PAGE and transferred to a polyvinylidene fluoride membrane. After blocking at room temperature with Blocking One (Nacalai Tesque), each membrane was incubated overnight at 4°C with the primary antibodies. After washing with TBS with Tween 20 (TBST), membranes were incubated with horseradish peroxidase (HRP)-conjugated secondary antibody for 1 hour at room temperature. Proteins of interest were visualized by enhanced chemiluminescence using ECL-Prime (GE Healthcare, Fairfield, CT, USA) and detected using ImageQuant LAS 4000 (GE Healthcare). Primary antibodies used in the experiments described in each figure are as follows: Actin: A2066 (Sigma-Aldrich), pAKT: #4060 (CST), AKT: #9272 (CST), pEGFR: #2234 (CST), EGFR: #4267 (CST), pERK: #4370 (CST), ERK: #9102 (CST)

***In vivo* xenograft studies**

All animal experimental procedures were approved by the Institutional Animal Care and Use Committee of Astellas Pharma Inc. Furthermore, Astellas Pharma Inc., Tsukuba Research Center has been awarded accreditation status by the Association for Assessment and Accreditation of Laboratory Animal Care International. HCC827, NCI-H1975, and A431 cells were inoculated subcutaneously into the flank of male CAnN.Cg-Foxn1nu/CrlCrlj mice. A xenograft study using LU1868 cells, a human NSCLC patient-derived xenograft (PDX) model with EGFR L858R/T790M, was conducted at Crown Bioscience Inc. LU1868 cells were inoculated subcutaneously into the flank of female BALB/c nude mice.

Mice were randomized and administered vehicle, naquotinib, erlotinib, or osimertinib at indicated doses (for details, see the figures for each experiment). Body weight and tumor diameter were measured twice a week, and tumor volume was determined by calculating the volume of an ellipsoid using the formula: length × width^2 × 0.5. All values are expressed as mean ± standard error of the mean (SEM).

Pharmacokinetics studies

Plasma and tumor concentrations of naquotinib were determined by high-performance liquid chromatography-tandem mass spectrometry (LC-MS/MS, Shimadzu 20AD LC System 2, Shimadzu Corporation and Triple Quad 5500, AB Sciex LLC). Naquotinib and deuterated naquotinib, used as an internal standard (IS), were added to 25 μL of mouse plasma and tumor homogenate containing 0.025% 2,2-dichlorovinyl dimethyl phosphate

(Wako Pure Chemical Industries, Ltd., Kyoto, Japan) with 300 μL of 0.5 mol/L $NaHCO_3$ solution (Kokusan Chemical Co., Ltd., Tokyo, Japan) and 3 mL of tert-butylm ethyl ether (Kanto Chemical Co., Inc., Tokyo, Japan), and the mixture was shaken and centrifuged. The organic layer was collected and evaporated to dryness under a stream of nitrogen gas at about 40°C. The residue was dissolved in 400 μL of 50 mmol/L NH_4HCO_3 buffer (Kanto Chemical Co., Inc.)/acetonitrile (Kokusan Chemical Co., Ltd.; 45:55, v/v), and 3 μL of the resulting solution was injected into the LC-MS/MS. The analytic column was a CAPCELL PAK C18 MGII (3.0 mm inner diameter × 75 mm, particle size 3 μm, Shiseido Co., Ltd., Tokyo, Japan) and the mobile phase comprised of 50 mmol/L NH_4HCO_3 buffer (45%) and acetonitrile (55%). The parent and product ions, m/z 563 and m/z 323 for naquotinib, and m/z 571 and m/z 323 for the IS, respectively, were monitored using positive multiple reaction monitoring. The IS method with peak area ratio was used to determine levels of naquotinib.

Measurement of EGFR phosphorylation in NCI-H1975 tumors

Phosphorylated EGFR and total EGFR were measured by sandwich ELISA assay using the DuoSet IC kit (DYC1095B and DYC1854, respectively; R&D Systems, Inc., Minneapolis, MN, USA). The assay was conducted in duplicate at room temperature. Chemiluminescence signals in ELISA were measured using an ARVO plate reader.

IHC of phosphorylated ERK in mouse skin

Tissue sections (4–5 μm thick) were deparaffinized and rehydrated. For antigen retrieval, sections were heated in 10 mmol/L sodium citrate buffer, pH 6.0 at 95°C for 10 minutes. Slides were washed with TBST three times and immersed in 3% H_2O_2 for 10 minutes at room temperature to quench endogenous peroxidases. Sections were treated with 5% goat serum used as a blocking agent for 1 hour at room temperature and then incubated with phosphorylated ERK (pERK) 1/2 rabbit mAb (CST) diluted with SignalStain Antibody Diluent (CST). Sections were washed with TBST three times for 5 minutes and treated with SignalStain Boost IHC Detection Reagent (HRP, Rabbit, CST) for 30 minutes at room temperature, before reacting with 3,30-diaminobenzidine at room temperature. Sections were counterstained with hematoxylin.

Results

In vitro activity of naquotinib on EGFR mutations and cancer cell lines

Naquotinib is a pyrazine carboxamide–based compound with a reactive acrylamide moiety. It is structurally different from other third-generation EGFR-TKIs such as osimertinib, rociletinib, and olmutinib, which have pyrimidine-based chemical structures (refs. 31–33; Fig. 1). *In vitro* biochemical enzymatic assays revealed that naquotinib inhibited EGFR del ex19, L858R, del ex19/T790M, and L858R/T790M with IC_{50} values of 5.5, 4.6, 0.26, and 0.41 nmol/L, respectively, and an IC_{50} value of 13 nmol/L against WT EGFR (Table 1). *In vitro* cell proliferation assays in human cancer cell lines harboring mutant EGFR or WT EGFR revealed that naquotinib inhibited the growth of NCI-H1975 (L858R/T790M), HCC827 (del ex19), PC-9 (del ex19), II-18 (L858R), A431 (WT), NCI-H292 (WT), and NCI-H1666 (WT) cells with IC_{50} values of 26, 7.3, 6.9, 43, 600, 260, and 230 nmol/L, respectively (Table 2). I further evaluated the inhibitory effect of naquotinib on EGFR and its downstream signals, ERK and AKT, by western blotting. Naquotinib dose-dependently suppressed the phosphorylation of EGFR, ERK, and AKT in HCC827 and NCI-H1975 cells at concentrations that showed antiproliferative effects in these cell lines. In contrast, the inhibitory effect of naquotinib on these molecules in A431 cells was weaker (Fig. 2A).

Naquotinib covalently binds to the cysteine-797 residue of EGFR L858R/T790M via its acrylamide moiety (34). I therefore investigated whether the covalent binding of naquotinib to mutant EGFR results in the prolonged inhibition of EGFR phosphorylation in NCI-H1975 cells by western blotting. Naquotinib continuously inhibited the phosphorylation of EGFR for at least 24 hours after removal of the compound (Fig. 2B).

In vivo antitumor activity of naquotinib in EGFR-mutant tumor models

The antitumor activity of naquotinib was evaluated in murine xenograft models using HCC827, NCI-H1975, and A431 cells and in a PDX model using LU1868 cells. In HCC827 and NCI-H1975 xenograft models, once-daily oral administration of naquotinib inhibited tumor growth with tumor regression at 10, 30, and 100 mg/kg (Fig. 3A and B) without affecting body weight (Fig. 4). In contrast, naquotinib did not significantly inhibit tumor growth at 10 and 30 mg/kg in an A431 xenograft model, but inhibited tumor growth at 100 mg/kg (Fig. 3C). These results indicate that naquotinib is selective for mutant EGFR in cell line xenograft models. In the PDX model using LU1868 (L858R/T790M) cells, erlotinib at 50 mg/kg did not inhibit tumor growth, which is in agreement with the resistance shown in clinical settings. In contrast, naquotinib significantly inhibited tumor growth at 10, 30, and 100 mg/kg, which is comparable with its effects in cell line xenograft models (Fig. 3B and D).

Naquotinib showed almost dose-proportional pharmacokinetics in both plasma and

tumors after a single oral dose of the compound in the NCI-H1975 xenograft model. Interestingly, naquotinib showed a higher concentration and a longer elimination half-life in tumors than plasma (Fig. 5A and B). Evaluation of the phosphorylation of EGFR in tumors under the same conditions confirmed that the inhibitory effect of naquotinib on EGFR phosphorylation in tumors also showed dose proportionality, and revealed that inhibition continued for at least 24 hours after dosing at 100 mg/kg (Fig. 5C). These data may suggest that, in addition to the irreversible covalent binding property of naquotinib, the retention of naquotinib in tumors also contributes to its prolonged EGFR inhibition in tumors.

Naquotinib spared inhibition of WT EGFR signaling in skin

To investigate the inhibitory effect of naquotinib, erlotinib, and afatinib on WT EGFR in skin, we conducted IHC staining for pERK in nude mice. Repeated dosing with erlotinib at 100 mg/kg and afatinib at 25 mg/kg eliminated the pERK signal in skin compared with nontreated controls. In contrast, naquotinib did not change the staining pattern of pERK even at 100 mg/kg (Fig. 6).

Discussion

In this study, I characterized the efficacy of naquotinib, a pyrazine carboxamide–based compound, as a third-generation EGFR-TKI. In *in vitro* experiments, naquotinib inhibited cell growth and EGFR signaling in NSCLC cell lines harboring mutant EGFR with or without T790M resistance mutation (Table 2). In xenograft models, naquotinib showed robust inhibition of tumor growth in NSCLC cell lines with EGFR mutations (Fig. 3A and B) and in a PDX model, which is thought to maintain intratumoral heterogeneity, indicating clinical efficacy in more than just monoclonal cell lines (Fig. 3D). These findings also suggest that naquotinib shows mutant selectivity and spares WT EGFR. Naquotinib inhibited cell growth and EGFR signaling in NSCLC cell lines harboring mutant EGFR with or without T790M more potently than those harboring WT EGFR *in vitro* (Fig. 2A and Table 2). IHC evaluation of EGFR signaling molecules in murine skin showed that erlotinib and afatinib inhibited the phosphorylation of ERK, which corresponds to the prevalence of severe skin rashes in clinical settings (11, 22). Naquotinib showed comparable mutant selectivity, sparing WT EGFR, to that of erlotinib *in vitro* (Table 2), and showed some inhibition of tumor growth in the A431 xenograft model (Fig. 3C). In contrast, naquotinib did not inhibit the phosphorylation of ERK in skin at 100 mg/kg (Fig. 6), the same dose that induced tumor regression in xenograft models with EGFR mutations (Fig. 3A, B, and D). Pharmacokinetic studies in the NCI-H1975 xenograft model showed that naquotinib had a higher concentration and a longer half-life in tumors than in plasma (Fig. 5A and B). This distribution may explain why naquotinib did not inhibit EGFR downstream signaling in skin. Considering that second-generation EGFR-TKIs are limited because of toxicity that likely arises from WT EGFR inhibition, the WT-sparing selectivity of naquotinib suggests that it may exert antitumor activity in patients with NSCLC harboring EGFR T790M resistance mutation without such limitations. This is in agreement with recent reports from naquotinib phase I–II clinical trials, in which skin toxicities were rarely observed (35).

In conclusion, naquotinib, a mutant-selective irreversible EGFR inhibitor, shows antitumor activity against NSCLC tumors that harbor EGFR-activating mutations, as well as EGFR T790M resistance mutation.

Figure 1. Chemical structures of naquotinib, osimertinib, rociletinib and olmutinib

Naquotinib

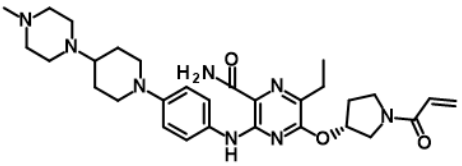

Rociletinib

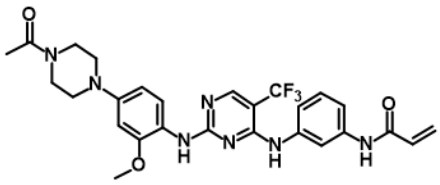

Osimertinib

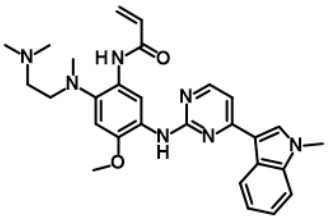

Olmutinib

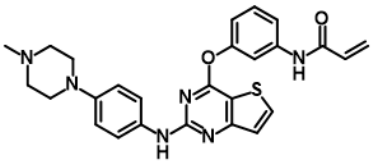

Figure 2. Inhibitory effect of naquotinib against EGFR and its downstream signaling molecules in cell lines.

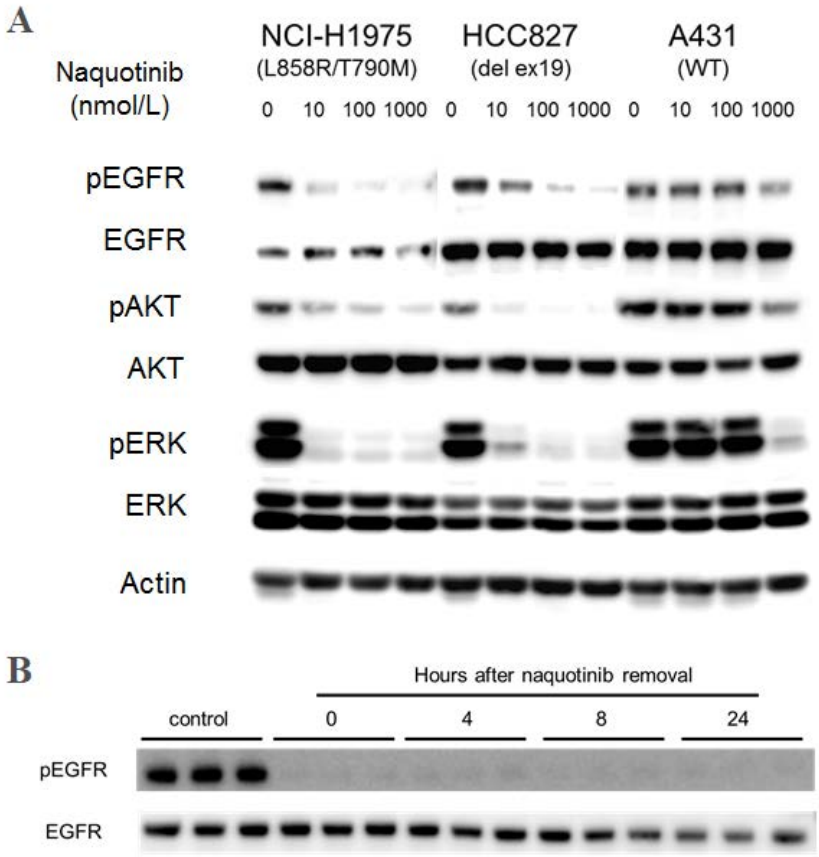

A, Inhibitory effect of naquotinib on the phosphorylation of EGFR and its downstream molecules ERK and AKT was evaluated in NCI-H1975 (L858R/T790M), HCC827 (del ex19), and A431 (WT) cells. Cells were treated with naquotinib for 4 hours and examined for the expression and phosphorylation of these molecules by western blotting. **B,** NCI-H1975 cells were exposed to 300 nmol/L naquotinib for 1 hour, washed with D-PBS(−), and cultured for 0, 4, 8, and 24 hours after removal of the compound. Phosphorylated EGFR (pEGFR) and EGFR protein levels were
detected by western blotting.

Figure 3. *In vivo* antitumor efficacy of naquotinib in subcutaneous xenograft models.

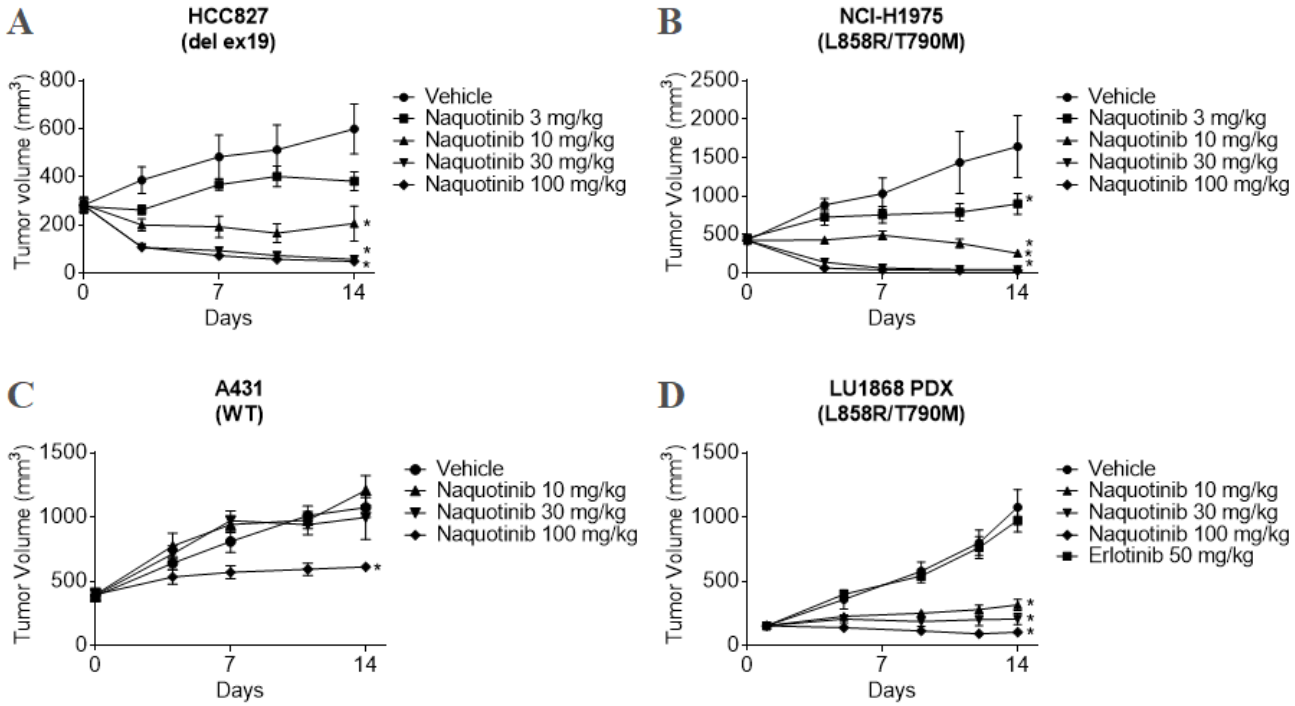

A, HCC827 (del ex19) xenograft model (n = 5). B, NCI-H1975 (L858R/T790M) xenograft model (n = 5). C, A431 (WT) xenograft model (n = 5). D, LU1868 (L858R/T790M) PDX model (n = 10). Mice were treated with vehicle, naquotinib, or erlotinib at the indicated doses for 14 days. Each datapoint represents the mean ± SEM. *, $P < 0.05$; **, $P < 0.01$ compared with the control group on day 14 (Dunnett test).

Figure 4. Naquotinib did not affect the body weight of mice in the NCI-H1975, HCC827 or A431 xenograft models

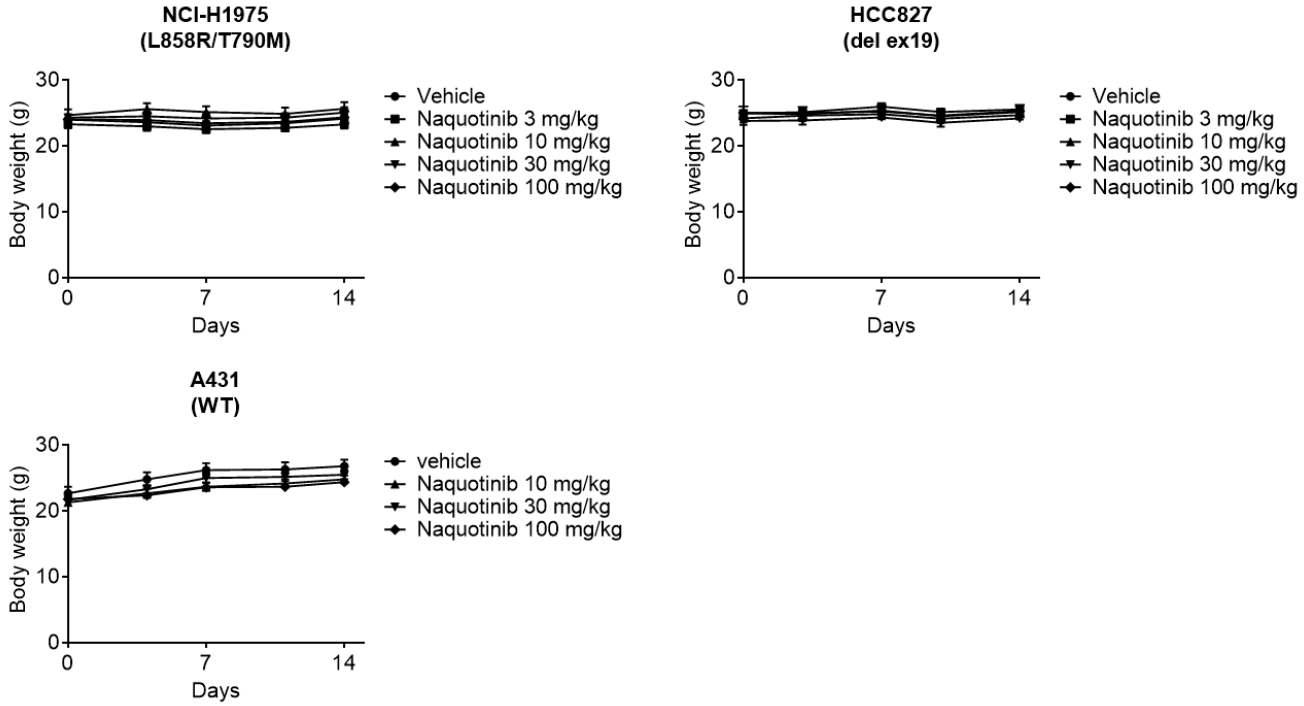

Mice were treated with vehicle or naquotinib at the indicated doses for 14 days. Each datapoint represents the mean ± SEM.

Figure 5. Pharmacokinetics and pharmacodynamics of naquotinib in the NCI-H1975 xenograft model

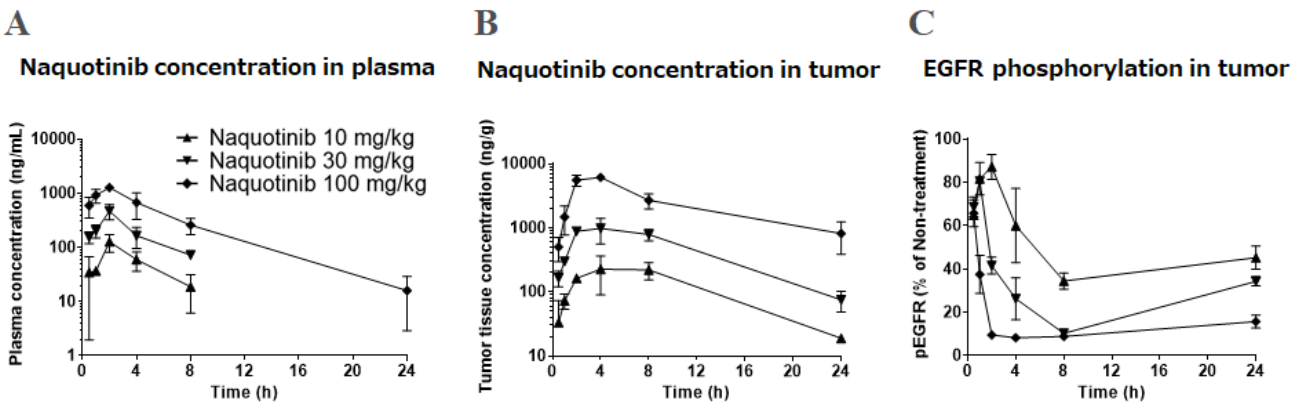

After single oral administration, naquotinib concentration was determined in plasma (A) and tumors (B) by LC-MS/MS. Each datapoint represents the mean ± SD (n = 3). C, Inhibitory effect of naquotinib on the phosphorylation of EGFR in tumors was evaluated by ELISA. Signals for phosphorylated EGFR (pEGFR) were normalized to those for EGFR. The percentage of pEGFR in each group relative to the control (nontreated) group was calculated. Each datapoint represents the mean ± SEM (n = 3).

Figure 6. IHC staining of phosphorylated ERK, a downstream molecule of EGFR

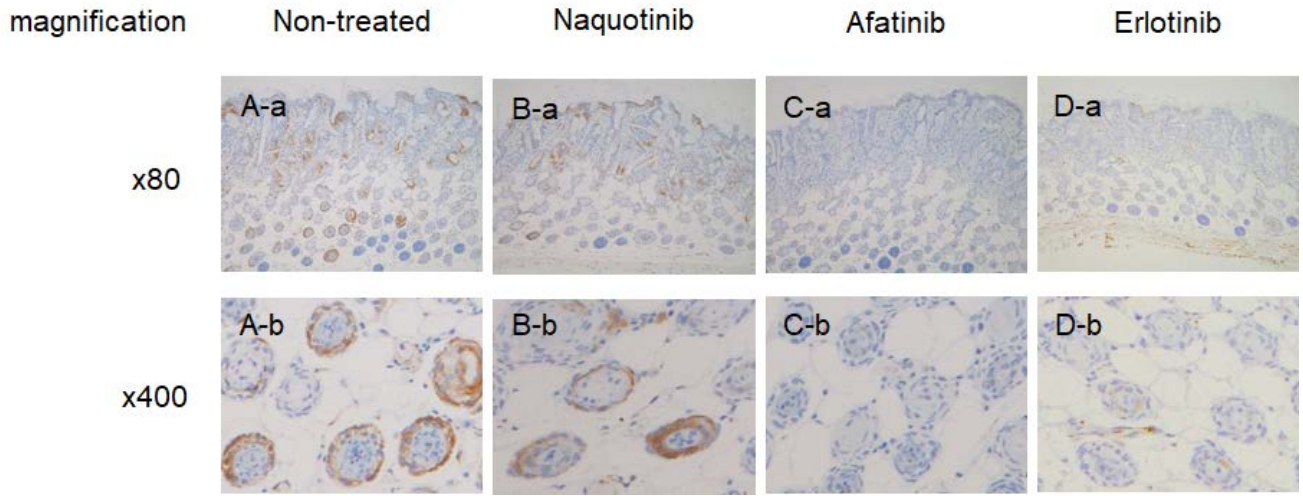

Nude mice were treated with EGFR-TKIs by oral administration over a 24-hour period. Three hours after the second treatment, the mice were sacrificed, and skin segments were dissected and fixed in 10% PBS-buffered formalin for 24 hours. The sections were subjected to IHC for phosphorylated ERK. A, Non-treated. B, Naquotinib 100 mg/kg. C, Afatinib 25 mg/kg. D, Erlotinib 100 mg/kg. Images were taken at a magnification of 80 × (a) or 400 × (b).

Table 1.

Inhibitory effect of naquotinib against wild-type or mutant EGFR kinase activity

IC_{50} (nmol/L)	G	del ex19 /T790M	L858R /T790M	del ex19	L858R	WT
Erlotinib	1	>10 uM	>10 uM	0.050	0.057	10
Afatinib	2	0.89	0.58	0.011	0.011	0.014
Naquotinib	**3**	**0.26**	**0.41**	**5.5**	**4.6**	**13**
Osimertinib	3	0.28	0.30	1.3	0.92	12

Table 2.

Inhibitory effect of naquotinib on the proliferation of cancer cell lines expressing mutant or WT EGFR

IC_{50} (nmol/L)	G	H1975	HCC827	PC-9	II-18	A431	H292	H1666
		L858R /T790M	del ex19	del ex19	L858R	WT	WT	WT
Erlotinib	1	>1000	9.8	6.6	81	530	270	48
Afatinib	2	230	0.76	3.0	0.88	39	21	2.8
Naquotinib	**3**	**26**	**7.3**	**6.9**	**43**	**600**	**260**	**230**
Osimertinib	3	28	4.3	2.5	21	340	160	110

NOTE: The IC_{50} value of each experiment was calculated using Sigmoid-Emax model nonlinear regression analysis and was expressed as the geometric mean of three independent experiments.

Chapter II: Profiling of Naquotinib, a Small Molecule Kinase Inhibitor, as BTK Inhibitor

Abstract

Diffuse large B-cell lymphoma (DLBCL), the most common type of B-cell non-Hodgkin lymphoma (NHL), is categorized into two major subtypes, activated B-cell-like (ABC) and germinal center B-cell-like (GCB). The ABC subtype is associated with worse prognosis than the GCB subtype using currently available therapies such as combination treatment with rituximab plus standard cytotoxic chemotherapy. The B-cell receptor (BCR) pathway is activated in ABC DLBCL, suggesting that inhibition of this pathway could provide an alternative strategy for treatment. Naquotinib is an irreversible tyrosine kinase inhibitor (TKI) originally designed to target the epidermal growth factor receptor (EGFR). As sequence alignment analysis indicates that irreversible EGFR-TKIs also inhibit Bruton's tyrosine kinase (BTK), here, I characterized the inhibitory effects of naquotinib against BTK in comparison to ibrutinib, acalabrutinib, tirabrutinib and spebrutinib. Naquotinib inhibited BTK kinase activity with similar potency to that for EGFR T790M mutation. *In vivo*, naquotinib induced tumor regression and suppressed tumor recurrence in TMD8 and OCI-Ly10, ABC DLBCL cell line xenograft models, at a lower dose than the clinically relevant dose. Compared to other BTK inhibitors, naquotinib showed faster onset and comparable inhibition of BTK following incubation with cell lines for 3 and 20 hours. In addition, naquotinib showed longer continuous inhibition of BTK following removal of the compound, lasting for at least 26 hours after removal. Pharmacokinetics studies in the TMD8 xenograft model showed higher concentration and slower elimination of naquotinib in tumors than other BTK inhibitors. These data suggest that naquotinib may have therapeutic potential in ABC DLBCL patients.

Introduction

Diffuse large B-cell lymphoma (DLBCL), an aggressive non-Hodgkin lymphoma (NHL), is the most common type of B-cell NHL, comprising approximately 30% of all NHLs (36). Gene expression profiling and immunohistochemistry have identified activated B-cell-like (ABC) and germinal center B-cell-like (GCB) as the two major biological subtypes of DLBCL (37–39). ABC DLBCL is thought to be derived from the differentiation of GCBs into plasmablastic cells, and these tumors have increased NF-kB activity and exhibit chronically active B-cell receptor (BCR) signaling. In contrast, GCB DLBCL is postulated to originate from GCBs, and these tumors have altered chromatin-modifying enzymes and phosphatidylinositol 3-kinase signaling (22).

The anti-CD20 antibody rituximab (Rituxan®) is commonly used to treat patients with multiple CD20-positive NHL, including DLBCL, and combination therapy comprising rituximab and standard cytotoxic chemotherapy regimens, such as R-CHOP (rituximab plus cyclophosphamide, hydroxydoxorubicin, vincristine, and prednisone), is the current standard of care for B-cell NHL (40–42). However, a subset of patients do not respond to this therapy, with some even developing resistance (43, 44). ABC DLBCL is more resistant to CHOP and R-CHOP than GCB DLBCL (23, 24).

Bruton's tyrosine kinase (BTK) is an essential kinase in the BCR signaling pathway and a driving force for several B-cell lymphoproliferative diseases (45–47). The first-generation BTK inhibitor ibrutinib has shown notable clinical activity against several B-cell malignancies with dependence on active BCR signaling, particularly mantle cell lymphoma (MCL), chronic lymphocytic leukemia (CLL) and Waldenstrom's macroglobulinemia (48–50). Although ABC DLBCL relies on BCR signaling and ibrutinib has been shown to exhibit antitumor activity in a non-clinical setting, ibrutinib has limited efficacy in relapsed/refractory (r/r) ABC DLBCL patients (51). Therefore, more potent BTK inhibitors are warranted. Naquotinib is a third-generation irreversible epidermal growth factor receptor (EGFR) tyrosine kinase inhibitor (TKI) that covalently binds to the cysteine-797 residue of EGFR (21). Naquotinib exhibits antitumor activity in preclinical models harboring EGFR activating mutations and T790M resistant mutation (52). Recent reports from open-label studies also suggest that naquotinib exhibits antitumor activity in non-small cell lung cancer (NSCLC) patients whose tumors harbor EGFR activating mutations as well as T790M resistance mutation (35).

Ten kinases, including BTK, resting lymphocyte kinase (RLK/TXK), and bone marrow kinase on the X chromosome (BMX), were previously predicted to possess a cysteine at the same position as EGFR. Several irreversible TKIs show cross-reactivity with these kinases (15, 53). In the present study, I evaluated the therapeutic potential of naquotinib as a BTK inhibitor for the treatment of ABC DLBCL.

Materials and Methods

Reagents

Naquotinib was prepared at Astellas Pharma Inc. Ibrutinib and tirabrutinib were synthesized according to the PCT Patent Applications WO2008/039218 and WO2013/081016, respectively. Acalabrutinib and spebrutinib were purchased from PharmaBlock Sciences (Nanjing), Inc. and Haoyuan Chemexpress Co., Ltd. (Shanghai), respectively.

In vitro kinase assays

The inhibitory effect of naquotinib against the kinase activities of BTK, BMX and TXK was investigated using the mobility shift assay at Carna Biosciences, Inc. (Kobe, Japan). Naquotinib was incubated with each kinase for 30 min at room temperature. After incubation, ATP and a substrate mixture were added to start the enzymatic reaction. The reaction mixture was examined using a LabChip EzReader II Screening System (PerkinElmer, Inc.) to separate and quantify the product and substrate peptide peaks.

Cell lines and cell culture

TMD8 was obtained from Tokyo Medical and Dental University (Tokyo, Japan) in 2014. OCI-Ly10 was obtained from The University Health Network (Toronto, Canada) in 2011. SU-DHL1, SU-DHL4, SU-DHL6, WSU-DLCL2 and JEKO-1 were obtained from Deutsche Sammlung von Mikroorganismen (Thüringen, Germany) in 2007, 2007, 2013, 2006 and 2008, respectively. SU-DHL10, REC1 and Mino were obtained from the American Type Culture Collection (Manassas, VA, USA) in 2013, 2013 and 2016, respectively. OCI-Ly10 cells were cultured in Iscove's Modified Dulbecco Minimum Essential Medium supplemented with 20% heat-inactivated fetal bovine serum at 37°C in a 5% CO_2 atmosphere. TMD8, SU-DHL1, SU-DHL4, SU-DHL6, SU-DHL10, WSU-DLCL2, REC1, JEKO-1 and Mino were cultured in RPMI1640 medium supplemented with 10% heat-inactivated fetal bovine serum at 37°C in a 5% CO_2 atmosphere. The cell lines used in this study were not authenticated in our laboratory but were purchased from the providers of authenticated cell lines and stored at early passages in a central cell bank at Astellas Pharma Inc. The experiments were conducted using low-passage cultures of these stocks with mycoplasma testing.

In vitro cell proliferation assays

OCI-Ly10 cells were plated at 1.0×10^4 cells/well; SU-DHL6 and Mino cells were plated at 5.0×10^3 cells/well; and TMD8, SU-DHL4, SU-DHL10, and REC1 cells were plated at 1.0×10^3 cells/well in 96-well white plates (Nunc 96 MicroWell™ Plates, White; Thermo Fisher Scientific, Waltham, MA, USA). Test compounds were added to the wells at final concentrations of 0.1, 0.3, 1, 3, 10, 30, 100, 300, 1000 and 3000 nmol/L and incubated

for 4 days. After treatment, the CellTiter-Glo® Luminescent Cell Viability Assay (Promega, Madison, WI, USA) was used according to the manufacturer's instructions and luminescence was measured using an ARVO plate reader (Perkin Elmer Inc., Waltham, MA). The assay was performed in triplicate. The effect of naquotinib on cell proliferation was analyzed using SAS software (SAS Institute Inc) or GraphPad Prism (GraphPad Software), and the IC_{50} value for each experiment was calculated using Sigmoid-Emax model non-linear regression analysis. The geometric mean was calculated from two individual experiments.

In vitro immunoblotting analysis

Protein was extracted using HTRF phospho-total lysis buffer (Cisbio Bioassays, Bedford, MA, U.S.A) or RIPA buffer (Thermo Fisher Scientific) supplemented with a phosphatase inhibitor cocktail (Thermo Fisher Scientific) and protease inhibitor cocktail (Sigma-Aldrich, St. Louis, MO, USA or Nacalai Tesque, Kyoto, Japan). Protein concentrations of the lysates were determined using the Pierce™ 660 nm Protein Assay Kit (Thermo Fisher Scientific). Equal amounts of total protein were resolved by SDS-PAGE and transferred to a polyvinylidene fluoride membrane. After blocking at room temperature with Blocking One (Nacalai Tesque), each membrane was incubated overnight at 4°C with primary antibodies against pBTK (#5082; Cell Signaling Technology (CST), Danvers, MA, USA), BTK (#3533; CST) and actin (A2066; Sigma-Aldrich). After washing with TBS with Tween 20 (TBST), membranes were incubated with horseradish peroxidase (HRP)-conjugated secondary antibody (Anti-rabbit IgG, HRP-linked Antibody, #7074; CST) for 1 hour at room temperature. Proteins of interest were visualized by enhanced chemiluminescence using ECL-Prime (GE Healthcare, Fairfield, CT, USA) and detected using ImageQuant LAS4000 (GE Healthcare).

In vivo xenograft studies

All animal experimental procedures were approved by the Institutional Animal Care and Use Committee of Astellas Pharma Inc. Furthermore, Astellas Pharma Inc., Tsukuba Research Center has been awarded Accreditation Status by the Association for Assessment and Accreditation of Laboratory Animal Care International. TMD8 or OCI-Ly10 cells were inoculated subcutaneously into the flank of female CB17/Icr-Prkdc^{scid}/CrlCrlj or NOD.CB17-Prkdc^{scid}/*J* mice, respectively.

Mice were randomized and administered vehicle, naquotinib, ibrutinib, acalabrutinib or tirabrutinibe at the indicated doses (for details, see the figure for each experiment). Body weight and tumor diameter were measured twice a week, and tumor volume was determined by calculating the volume of an ellipsoid using the formula length × width^2 × 0.5. All values are expressed as mean ± standard error of the mean (SEM). The data were statistically analyzed using Dunnett's multiple comparison test or Student's *t*-test with GraphPad Prism (GraphPad Software, San Diego, CA, USA).

Pharmacokinetics studies

The assay method used to determine plasma and tumor concentrations of naquotinib has been described in chapter I. To determine the concentrations of unchanged ibrutinib, acalabrutinib and tirabrutinib in plasma and tumor tissue, blood and tumor samples were collected from xenograft mice after a single oral administration. The plasma was separated using centrifugation, and tumor tissue was homogenized in PBS. The samples were subjected to protein precipitation, and the supernatant was analyzed using high-performance liquid chromatography-tandem mass spectrometry (LC–MS/MS).

Results

In vitro activity of naquotinib against BTK and B-cell lymphoma cell lines

I evaluated the inhibitory effect of naquotinib against BTK, TXK, and BMX kinases, all of which possess a cysteine at the same position as that in EGFR. *In vitro* biochemical enzymatic assays revealed that naquotinib inhibited BTK, TXK and BMX with IC_{50} values of 0.23, 0.27 and 0.65 nmol/L, respectively (Table 3).

Naquotinib covalently binds to the cysteine-481 residue of BTK (34), probably via its acrylamide moiety. *In vitro* cellular inhibitory assay using western blotting showed that naquotinib dose-dependently suppressed auto-phosphorylation of BTK in TMD8 cells (Fig. 7). Compared to the other BTK inhibitors, naquotinib showed faster onset and comparable inhibition following incubation with the cell line for 3 and 20 hours. I also evaluated whether the covalent binding of naquotinib to BTK results in prolonged inhibition of BTK auto-phosphorylation in TMD8 cells by western blotting. Naquotinib continuously inhibited auto-phosphorylation of BTK for at least 26 hours after removal of the compound (Fig. 8). Interestingly, naquotinib showed the longest continuous inhibition among the tested BTK inhibitors.

In the *in vitro* cell proliferation assay, naquotinib showed similar selectivity to the other BTK inhibitors for inhibiting the growth of human B-cell lymphoma cell lines (54, 55). Naquotinib inhibited the growth of TMD8 (ABC DLBCL), OCI-Ly10 (ABC DLBCL), REC1 (MCL) and JEKO-1 (MCL) cells with IC_{50} values of 0.90, 1.0, 1.3 and 6.6 nmol/L, respectively (Table 4). In contrast, naquotinib inhibited the growth of SU-DHL1 (GCB DLBCL), SU-DHL4 (GCB DLBCL), SU-DHL6 (GCB DLBCL), SU-DHL10 (GCB DLBCL), WSU-DLCL2 (GCB DLBCL) and Mino (MCL) cells with IC_{50} values of 110, 450, 330, 300, 340 and 570 nmol/L, respectively.

In vivo antitumor activity of naquotinib in ABC DLBCL tumor models

The antitumor activity of naquotinib was evaluated in murine xenograft models using TMD8 and OCI-Ly10 cells. In these xenograft models, twice-daily oral administration of naquotinib at 30 and 100 mg/kg significantly inhibited tumor growth with tumor regression (TMD8: 64% and 78% regression, respectively, $P < 0.01$ on Day14; OCI-Ly10: 90% and 91% regression, respectively, $P < 0.01$ on Day 28), and induced sustained tumor regression during the treatment period of 28 days, with no signs of recurrence (Figs. 9 and 10) and no effect on body weight (Fig. 11). While ibrutinib at 100 mg/kg also induced sustained tumor regression in the OCI-Ly10 xenograft model during the treatment period, it did not result in complete regression in the TMD-8 xenograft model. Administration of ibrutinib at 30 mg/kg in both models resulted in tumor regrowth despite treatment. Similarly, acalabrutinib and tirabrutinibe at 30 and 100 mg/kg resulted in regrowth in both xenograft models despite treatment.

Pharmacokinetics studies

After single oral administration of naquotinib to TMD8 xenograft model mice, the exposure in plasma and tumor increased with increasing dose. Interestingly, higher concentration and slower elimination of naquotinib was observed in tumors than in plasma (Fig. 12). In contrast, other BTK inhibitors showed lower and shorter exposure than naquotinib.

Discussion

In this study, I evaluated the efficacy of naquotinib as a BTK inhibitor. In *in vitro* experiments, naquotinib inhibited BTK kinase activity with similar potency to that for EGFR activating mutations (Table 3) and showed selective inhibition of cell growth that was dependent on chronically active BCR signaling among B-cell lymphoma cells, such as ABC DLBCL and MCL (Table 4) (54, 55). In ABC DLBCL xenograft models, naquotinib at 30 and 100 mg/kg produced sustained tumor regression with no signs of recurrence in TMD8 and OCI-Ly10 cells. In contrast, among the other BTK inhibitors, only ibrutinib at 100 mg/kg resulted in tumor regression with no sign of recurrence (Figs. 9 and 10). Pharmacokinetics analysis using the AUC of the fraction unbound (f_u) indicated that the estimated clinically relevant dose of naquotinib in the TMD8 xenograft model was 64 mg/kg/day based on data in NSCLC patients who responded to treatment with naquotinib (data not shown). I also confirmed that the clinically relevant dose of ibrutinib, acalabrutinib and tirabrutinibe was comparable to that of naquotinib (data not shown). This result suggests that naquotinib induced tumor regression in TMD8 and OCI-Ly10 models at a lower dose than the clinically relevant dose. Collectively, these data suggest that naquotinib may have potential antitumor activity in ABC DLBCL patients. However, further investigations, such as those in patient-derived xenograft (PDX) models, are expected to strengthen the rationale for future clinical studies in ABC DLBCL.

I also showed that naquotinib has some unique features compared to currently available BTK inhibitors and those in clinical trials. In *in vitro* immunoblotting analysis, naquotinib showed faster onset of inhibition of BTK phosphorylation and continuous inhibition following removal of the compound (Fig. 8). In contrast, other BTK inhibitors showed insufficient inhibition at 3 hours and attenuation after removal. Pharmacokinetics studies in the TMD8 xenograft model showed higher concentration and slower elimination of naquotinib in tumors than in plasma (Fig. 12). In contrast, other BTK inhibitors showed lower and shorter exposure in tumors than naquotinib. Physiologically based pharmacokinetics modeling suggests that antitumor basic drugs have high affinity for acidic phospholipids tumor (56, 57). Given that naquotinib is a pyrazine carboxamide-based compound and displays basicity, this polarity and the covalent binding property of naquotinib may contribute to its retention and prolonged inhibition of BTK in tumors.

In conclusion, naquotinib inhibited BTK and exhibited antitumor activity against ABC DLBCL *in vitro* and *in vivo*. These findings suggest that naquotinib has therapeutic potential in the treatment of ABC DLBCL.

Fig. 7. Inhibitory effect of naquotinib against BTK in TMD8 cells

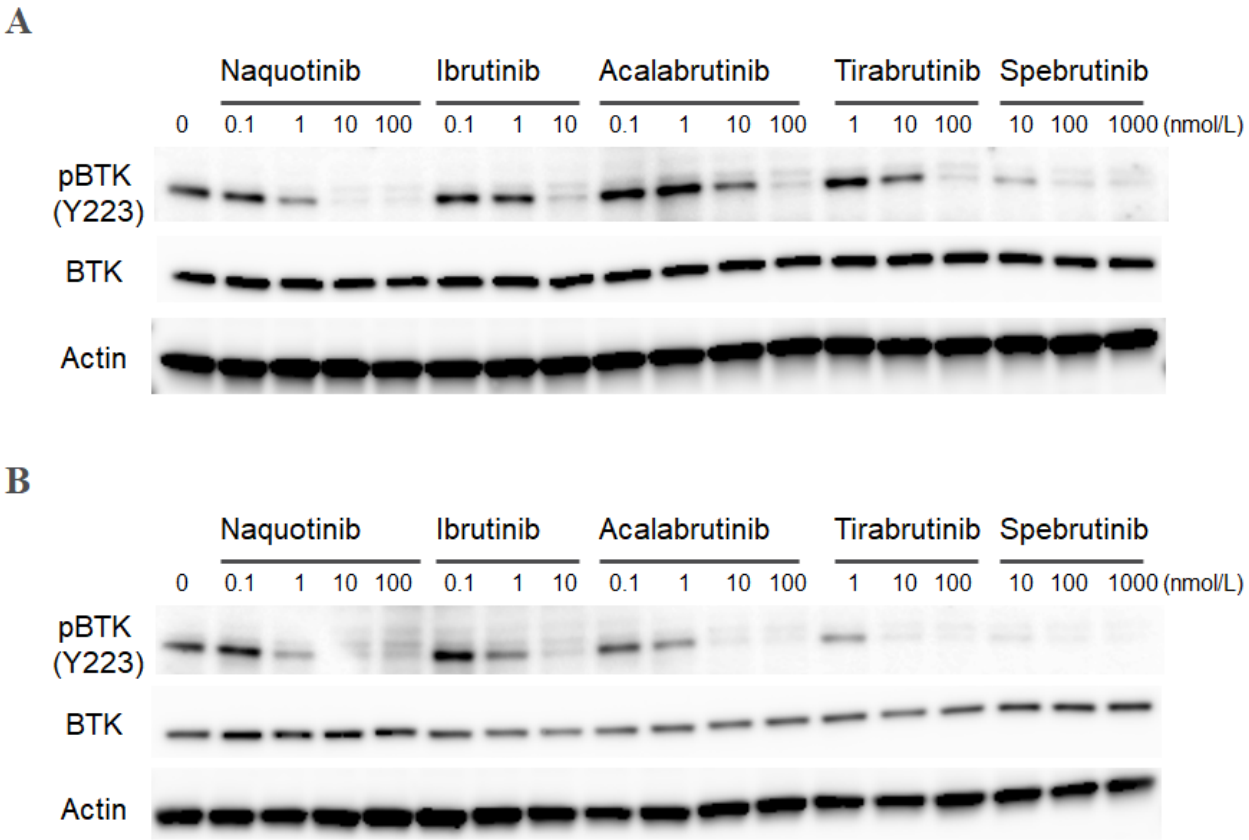

TMD8 cells were treated with DMSO, increasing concentrations of naquotinib, or the indicated BTK inhibitors for 3 (A) or 20 hours (B) and examined by western blotting for expression and phosphorylation of BTK.

Fig. 8. Time course of BTK phosphorylation in TMD8 cells after removal of the compounds

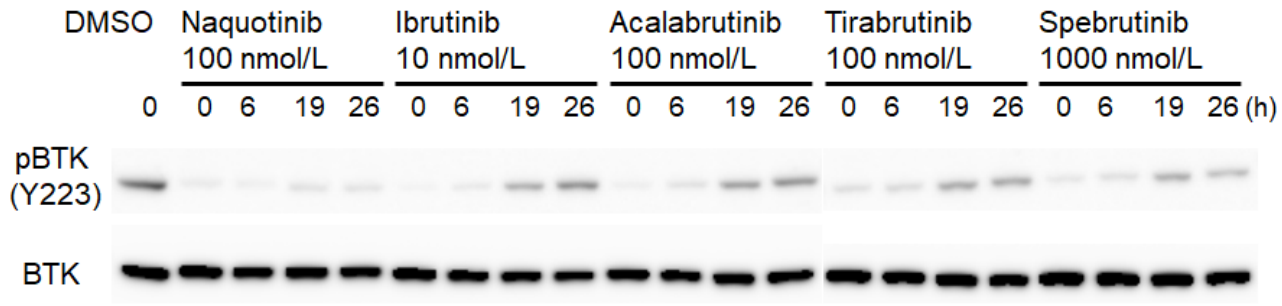

TMD8 cells were exposed to various compounds at the indicated concentrations for 3 hours, washed with D-PBS(−), and cultured for 0, 6, 19, and 26 hours after removal of the compounds. Phosphorylated BTK (pBTK) and BTK protein levels were subsequently examined by western blotting.

Fig. 9. Antitumor activity of naquotinib and BTK inhibitors in the TMD8 xenograft model

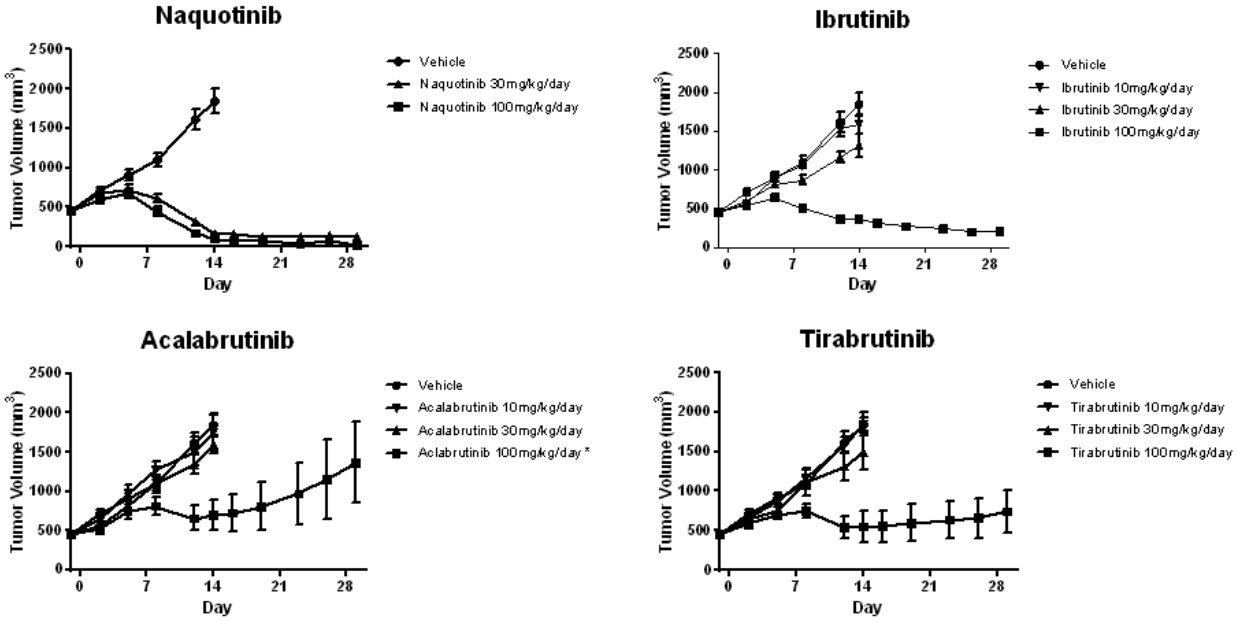

Mice were twice-daily orally treated with vehicle, naquotinib or BTK inhibitors at the indicated doses for 28 days. Each point represents the mean ± SEM (n=5 or #4). *, $P < 0.05$; **, $P < 0.01$ compared with vehicle on Day 14 (Dunnett's test).

Fig. 10. Antitumor activity of naquotinib and BTK inhibitors in the OCI-Ly10 xenograft model

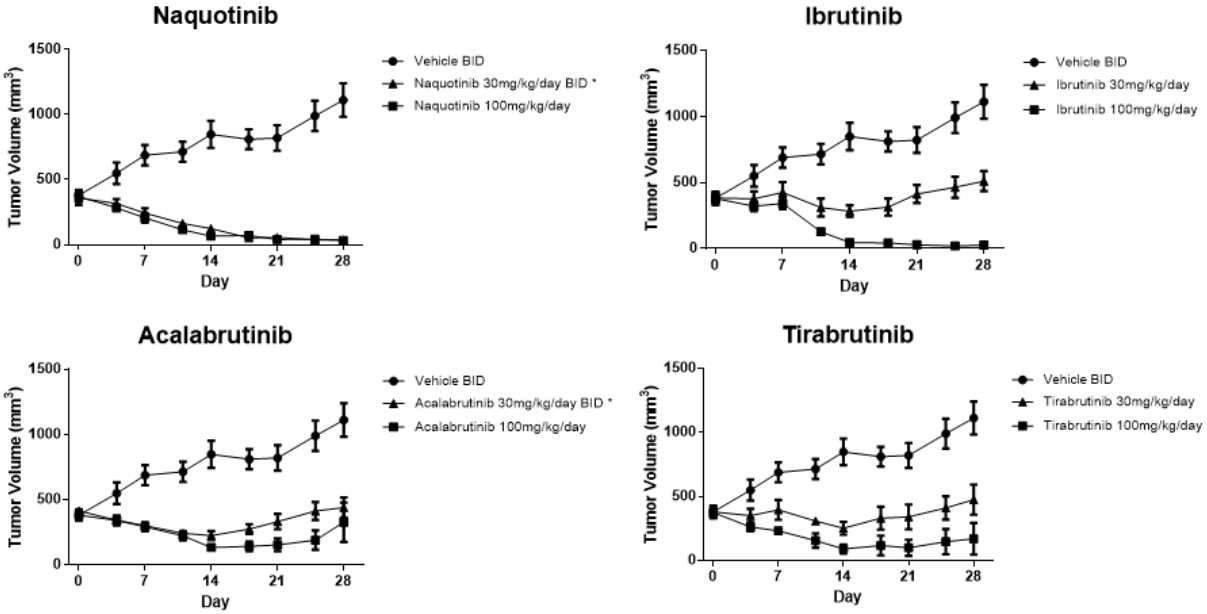

Mice were twice-daily orally treated with vehicle, naquotinib or BTK inhibitors at the indicated doses for 28 days. Each point represents the mean ± SEM (n=5 or #4). **, $P < 0.01$ compared with vehicle on Day 28 (Dunnett's test).

Fig. 11. Naquotinib did not affect the body weight of mice in the TMD8 or OCI-Ly10 xenograft models

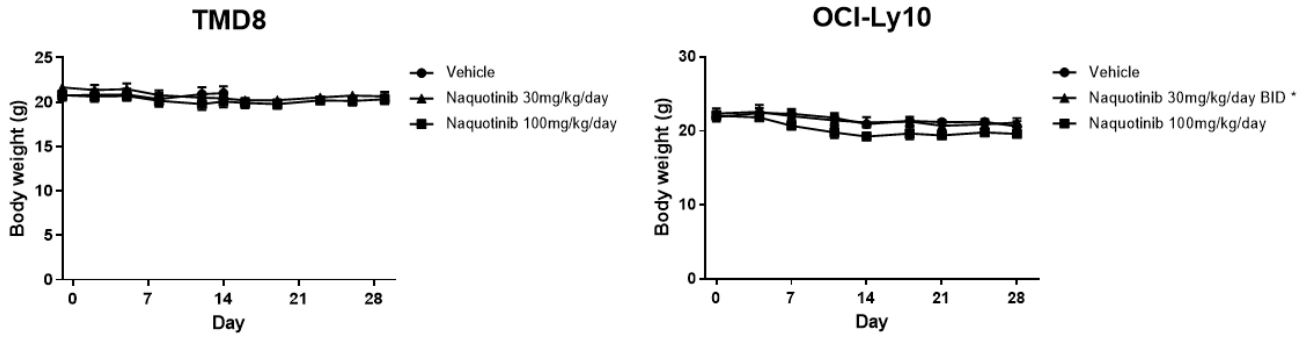

Mice were twice-daily orally treated with vehicle or naquotinib at the indicated doses for 28 days. Each point represents the mean ± SEM (n=5 or #4).

Fig. 12. Pharmacokinetics of naquotinib and BTK inhibitors in the TMD8 xenograft model

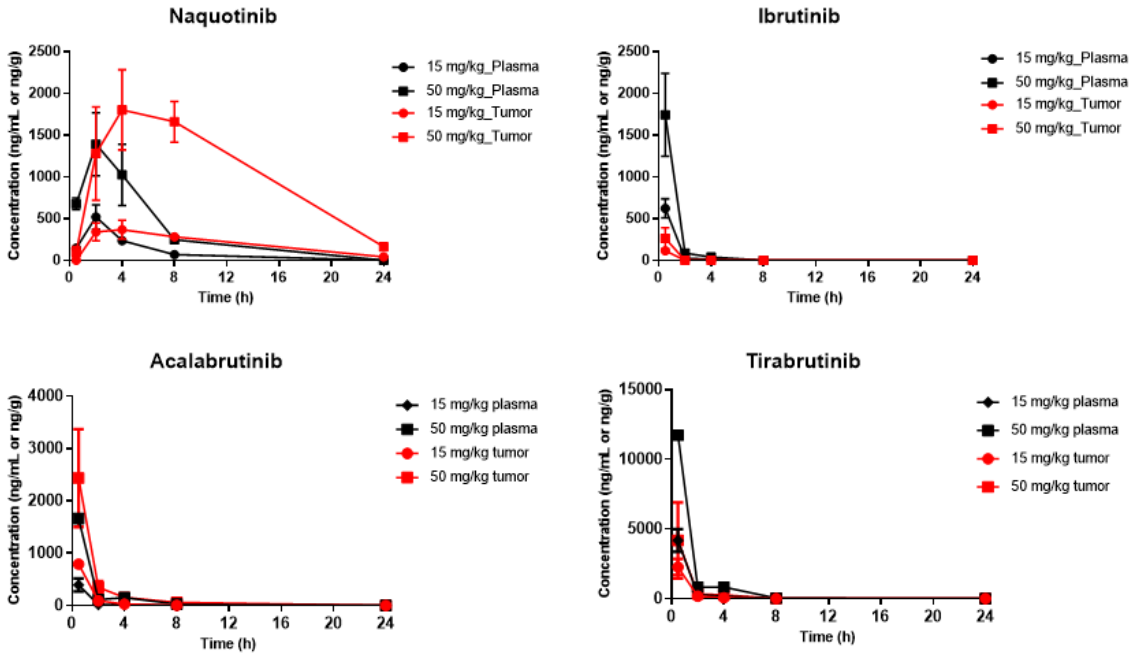

Mice were orally treated with naquotinib or BTK inhibitors, and plasma and tumor tissue were collected at 0.5, 2, 4, 8, and 24 hours after treatment. Data are presented as mean ± SD (n=3).

Table 3. Inhibitory effect of naquotinib against the TEC family of kinases

IC_{50} (nmol/L)	BTK	TXK	BMX	EGFR [del ex19/T790M]	EGFR [L858R/T790M]
Naquotinib	**0.23**	**0.27**	**0.65**	**0.26**	**0.41**

Table 4. Anti-proliferative activity against B-cell lymphoma cells.

IC_{50} (nmol/L)	TMD8	OCI-Ly10	SU-DHL4	SU-DHL6	SU-DHL10	REC1	Mino
Origin	DLBCL	DLBCL	DLBCL	DLBCL	DLBCL	MCL	MCL
Naquotinib	**0.90**	**1.0**	**450**	**330**	**300**	**1.3**	**570**
Ibrutinib	0.33	1.4	1200	86	570	0.18	>3000
Acalabrutinib	2.8	6.3	>3000	>10000	>2800	2.6	>3000
Tirabrutinib	4.6	9.4	>2800	2800	>2600	6.6	>2800
Spebrutinib	22	19	>3000	2700	970	21	1200

The IC_{50} values in this table indicate the geometric mean of two individual experiments.

General Discussion

In this study, I characterized the profile of naquotinib, a covalent TKI inhibitor, as EGFR inhibitor (Chapter I) and as BTK inhibitor (Chapter II) using molecular biological, pharmacological and pharmacokinetic methods, including *in vitro* enzyme inhibition assays, *in vitro* cell proliferation assays, and *in vivo* xenograft studies. In *in vitro* experiments, naquotinib inhibited EGFR T790M resistant kinase activity and BTK kinase activity with similar potency (Tables 1 and 3). In addition, naquotinib inhibited NSCLC cell lines harboring mutant EGFR and B-cell lymphoma cell lines depending on chronically active BCR signaling (Tables 2 and 4). In *in vivo* experiments, naquotinib showed robust inhibition of tumor growth both in NSCLC cell lines with EGFR mutations and in ABC DLBCL cell lines (Figs. 3, 9 and 10). Pharmacokinetic studies in both EGFR and ABC DLBCL xenograft model showed that naquotinib had a higher concentration and a longer half-life in tumors than in plasma (Figs. 5 and 12). These findings suggest that when the inhibitor demonstrates an inhibitory activity comparable to that of the target enzyme, it has comparable cell proliferation inhibitory activity, antitumor activity, and biodistribution.

I also showed that naquotinib had target-selective inhibition. Naquotinib inhibited NSCLC cell lines harboring mutant EGFR with or without T790M more potently than those harboring WT EGFR, and B-cell lymphoma cell lines depending on chronically active BCR signaling more potently than others (Tables 2 and 4). In addition, naquotinib did not affect body weight in *in vivo* xenograft models and did not show noteworthy side effects in phase I–II clinical trials (35). A comprehensive kinase panel evaluation revealed that naquotinib inhibited only a few enzymes other than EGFR and BTK (21).

I will consider this enzyme selectivity. *In silico* structural analysis revealed that naquotinib inhibited EGFR and BTK in a very similar manner. Naquotinib binds covalently to a cysteine residue near the gatekeeper amino acid, forms hydrogen-bonds with the hinge region, and occupies space near the gatekeeper with both EGFR and BTK enzymes (Fig. 13). In the first place, the gatekeeper is identified as the amino acid that contributes most to enzyme activity, located in the innermost part of the ATP binding pocket. In other words, it has been clarified that the most important space for inhibiting enzyme activity exists near the gatekeeper. These give me thought that the positional relationship between the gatekeeper amino acid and the cysteine residue, which naquotinib bond covalently, is important for inhibition activity. *In silico* structural analysis revealed that ten kinases, including EGFR and BTK, were predicted to possess a cysteine at the same position as EGFR (15). Surprisingly, naquotinib did not show strong inhibitory activity against enzymes other than these 10 enzymes (21). In other words, naquotinib acquired superior kinase selectivity for all kinases except for such special kinases.

In this study, I have shown that increasing enzyme selectivity can create powerful yet

safe covalent enzyme inhibitors. This opens the way for the creation of inhibitors not only for resistant mutant enzymes but also for targets that could not be inhibited by competitive inhibitors, such as having no definite pocket structure.

Figure 13. Binding pose of naquotinib with EGFR and BTK.

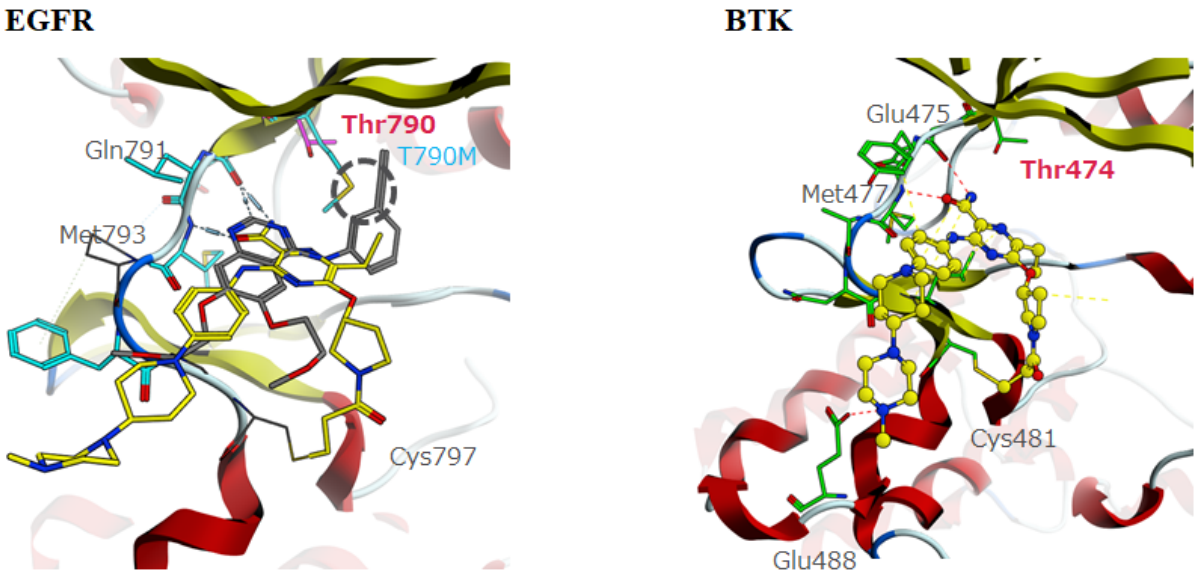

The EGFR or BTK kinase is shown in a ribbon representation (α-helix: red, β-sheet: yellow). Naquotinib (yellow) or erlotinib (gray) is shown in a licorice or ball-and-stick model. Acrylamide moiety forms of naquotinib forms a covalent bond with Cys797 of the EGFR kinase (left), and Cys481 of the BTK kinase (right). Naquotinb forms hydrogen bonds with Gln791 and Met793 (gray dashed lines) of the EGFR kinase (left), and with Glu475, Met477 and Glu488 (red dashed lines) of the BTK kinase (right).

Acknowledgments

I am deeply grateful to Associate Professor Kazuichi Sakamoto of the University of Tsukuba for his guidance and valuable discussions in the doctoral program. I am also grateful to Associate Professor Ryuhei Harada, Associate Professor Kyoichi Sawamura and Assistant Professor Fuminori Tsuruta for their valuable suggestions and helpful supports.

I would also like to thank Dr. Taku Yoshida and Dr. Kenna Shirasuna of Astellas Pharma Inc. for their understanding and supporting for my doctoral program.

Finally, I would like to thank my family for supporting my time at the University of Tsukuba.

References

1. Zamecnikova A. Novel approaches to the development of tyrosine kinase inhibitors and their role in the fight against cancer. Expert opinion on drug discovery **2014**;9:77-92

2. Huang L, Jiang S, Shi Y. Tyrosine kinase inhibitors for solid tumors in the past 20 years (2001-2020). Journal of hematology & oncology **2020**;13:143

3. Lynch TJ, Bell DW, Sordella R, Gurubhagavatula S, Okimoto RA, Brannigan BW, *et al.* Activating mutations in the epidermal growth factor receptor underlying responsiveness of non-small-cell lung cancer to gefitinib. The New England journal of medicine **2004**;350:2129-39

4. Marchetti A, Martella C, Felicioni L, Barassi F, Salvatore S, Chella A, *et al.* EGFR mutations in non-small-cell lung cancer: analysis of a large series of cases and development of a rapid and sensitive method for diagnostic screening with potential implications on pharmacologic treatment. Journal of clinical oncology : official journal of the American Society of Clinical Oncology **2005**;23:857-65

5. Kosaka T, Yatabe Y, Endoh H, Kuwano H, Takahashi T, Mitsudomi T. Mutations of the epidermal growth factor receptor gene in lung cancer: biological and clinical implications. Cancer research **2004**;64:8919-23

6. Mok TS, Wu YL, Thongprasert S, Yang CH, Chu DT, Saijo N, *et al.* Gefitinib or carboplatin-paclitaxel in pulmonary adenocarcinoma. The New England journal of medicine **2009**;361:947-57

7. Cappuzzo F, Ciuleanu T, Stelmakh L, Cicenas S, Szczesna A, Juhasz E, *et al.* Erlotinib as maintenance treatment in advanced non-small-cell lung cancer: a multicentre, randomised, placebo-controlled phase 3 study. The Lancet Oncology **2010**;11:521-9

8. Sequist LV, Yang JC, Yamamoto N, O'Byrne K, Hirsh V, Mok T, *et al.* Phase III study of afatinib or cisplatin plus pemetrexed in patients with metastatic lung adenocarcinoma with EGFR mutations. Journal of clinical oncology : official journal of the American Society of Clinical Oncology **2013**;31:3327-34

9. Janne PA, Ou SH, Kim DW, Oxnard GR, Martins R, Kris MG, *et al.* Dacomitinib as first-line treatment in patients with clinically or molecularly selected advanced non-small-cell lung cancer: a multicentre, open-label, phase 2 trial. The Lancet Oncology **2014**;15:1433-41

10. Kobayashi S, Boggon TJ, Dayaram T, Janne PA, Kocher O, Meyerson M, *et al.* EGFR mutation and resistance of non-small-cell lung cancer to gefitinib. The New England journal of medicine **2005**;352:786-92

11. Blakely CM, Bivona TG. Resiliency of lung cancers to EGFR inhibitor treatment unveiled,

offering opportunities to divide and conquer EGFR inhibitor resistance. Cancer discovery **2012**;2:872-5

12. Sequist LV, Waltman BA, Dias-Santagata D, Digumarthy S, Turke AB, Fidias P, *et al.* Genotypic and histological evolution of lung cancers acquiring resistance to EGFR inhibitors. Science translational medicine **2011**;3:75ra26

13. Yu HA, Arcila ME, Rekhtman N, Sima CS, Zakowski MF, Pao W, *et al.* Analysis of tumor specimens at the time of acquired resistance to EGFR-TKI therapy in 155 patients with EGFR-mutant lung cancers. Clinical cancer research : an official journal of the American Association for Cancer Research **2013**;19:2240-7

14. Yun CH, Mengwasser KE, Toms AV, Woo MS, Greulich H, Wong KK, et al. The T790M mutation in EGFR kinase causes drug resistance by increasing the affinity for ATP. Proceedings of the National Academy of Sciences of the United States of America **2008**;105:2070-5

15. Zhou W, Ercan D, Chen L, Yun CH, Li D, Capelletti M, *et al.* Novel mutant-selective EGFR kinase inhibitors against EGFR T790M. Nature **2009**;462:1070-4

16. Mok TS, Wu YL, Ahn MJ, Garassino MC, Kim HR, Ramalingam SS, *et al.* Osimertinib or Platinum-Pemetrexed in EGFR T790M-Positive Lung Cancer. The New England journal of medicine **2017**;376:629-40

17. Sequist LV, Soria JC, Goldman JW, Wakelee HA, Gadgeel SM, Varga A, *et al.* Rociletinib in EGFR-mutated non-small-cell lung cancer. The New England journal of medicine **2015**;372:1700-9

18. Park K, Lee JS, Han JY, Lee KH, Kim JH, Cho EK, *et al.* 1300: Efficacy and safety of BI 1482694 (HM61713), an EGFR mutant-specific inhibitor, in T790M-positive NSCLC at the recommended phase II dose. Journal of thoracic oncology : official publication of the International Association for the Study of Lung Cancer **2016**;11:S113

19. Schuler M, Yang JC, Park K, Kim JH, Bennouna J, Chen YM, *et al.* Afatinib beyond progression in patients with non-small-cell lung cancer following chemotherapy, erlotinib/gefitinib and afatinib: phase III randomized LUX-Lung 5 trial. Annals of oncology : official journal of the European Society for Medical Oncology **2016**;27:417-23

20. Wu YL, Cheng Y, Zhou X, Lee KH, Nakagawa K, Niho S, *et al.* Dacomitinib versus gefitinib as first-line treatment for patients with EGFR-mutation-positive non-small-cell lung cancer (ARCHER 1050): a randomised, open-label, phase 3 trial. The Lancet Oncology **2017**;18:1454-66

21. Hirano T, Yasuda H, Hamamoto J, Nukaga S, Masuzawa K, Kawada I, *et al.* Pharmacological and Structural Characterizations of Naquotinib, a Novel Third-Generation EGFR Tyrosine

Kinase Inhibitor, in EGFR-Mutated Non-Small Cell Lung Cancer. Molecular cancer therapeutics **2018**;17:740-50

22. Basso K, Dalla-Favera R. Germinal centres and B cell lymphomagenesis. Nature reviews Immunology **2015**;15:172-84

23. Fu K, Weisenburger DD, Choi WW, Perry KD, Smith LM, Shi X, *et al.* Addition of rituximab to standard chemotherapy improves the survival of both the germinal center B-cell-like and non-germinal center B-cell-like subtypes of diffuse large B-cell lymphoma. Journal of clinical oncology : official journal of the American Society of Clinical Oncology **2008**;26:4587-94

24. Roschewski M, Staudt LM, Wilson WH. Diffuse large B-cell lymphoma-treatment approaches in the molecular era. Nature reviews Clinical oncology **2014**;11:12-23

25. Hsuan JJ, Tan SH. Growth factor-dependent phosphoinositide signalling. The international journal of biochemistry & cell biology **1997**;29:415-35

26. Burgering BM, Coffer PJ. Protein kinase B (c-Akt) in phosphatidylinositol-3-OH kinase signal transduction. Nature **1995**;376:599-602

27. Herbst RS, Heymach JV, Lippman SM. Lung cancer. The New England journal of medicine **2008**;359:1367-80

28. Wells A. EGF receptor. The international journal of biochemistry & cell biology **1999**;31:637-43

29. Rosell R, Moran T, Queralt C, Porta R, Cardenal F, Camps C, *et al.* Screening for epidermal growth factor receptor mutations in lung cancer. The New England journal of medicine **2009**;361:958-67

30. Sharma SV, Bell DW, Settleman J, Haber DA. Epidermal growth factor receptor mutations in lung cancer. Nature reviews Cancer **2007**;7:169-81

31. Finlay MR, Anderton M, Ashton S, Ballard P, Bethel PA, Box MR, *et al.* Discovery of a potent and selective EGFR inhibitor (AZD9291) of both sensitizing and T790M resistance mutations that spares the wild type form of the receptor. Journal of medicinal chemistry **2014**;57:8249-67

32. Walter AO, Sjin RT, Haringsma HJ, Ohashi K, Sun J, Lee K, *et al.* Discovery of a mutant-selective covalent inhibitor of EGFR that overcomes T790M-mediated resistance in NSCLC. Cancer discovery **2013**;3:1404-15

33. Kim ES. Olmutinib: First Global Approval. Drugs **2016**;76:1153-7

34. Anastassiadis T, Deacon SW, Devarajan K, Ma H, Peterson JR. Comprehensive assay of kinase catalytic activity reveals features of kinase inhibitor selectivity. Nature biotechnology **2011**;29:1039-45

35. Yu HA, Spira A, Horn L, Weiss J, West H, Giaccone G, *et al.* A Phase I, Dose Escalation Study of Oral ASP8273 in Patients with Non-small Cell Lung Cancers with Epidermal Growth Factor Receptor Mutations. Clinical cancer research : an official journal of the American Association for Cancer Research **2017**;23:7467-73

36. A clinical evaluation of the International Lymphoma Study Group classification of non-Hodgkin's lymphoma. The Non-Hodgkin's Lymphoma Classification Project. Blood **1997**;89:3909-18

37. Alizadeh AA, Eisen MB, Davis RE, Ma C, Lossos IS, Rosenwald A, *et al.* Distinct types of diffuse large B-cell lymphoma identified by gene expression profiling. Nature **2000**;403:503-11

38. Hans CP, Weisenburger DD, Greiner TC, Gascoyne RD, Delabie J, Ott G, *et al.* Confirmation of the molecular classification of diffuse large B-cell lymphoma by immunohistochemistry using a tissue microarray. Blood **2004**;103:275-82

39. Read JA, Koff JL, Nastoupil LJ, Williams JN, Cohen JB, Flowers CR. Evaluating cell-of-origin subtype methods for predicting diffuse large B-cell lymphoma survival: a meta-analysis of gene expression profiling and immunohistochemistry algorithms. Clinical lymphoma, myeloma & leukemia **2014**;14:460-7.e2

40. Coiffier B, Lepage E, Briere J, Herbrecht R, Tilly H, Bouabdallah R, *et al.* CHOP chemotherapy plus rituximab compared with CHOP alone in elderly patients with diffuse large-B-cell lymphoma. The New England journal of medicine **2002**;346:235-42

41. Griffin MM, Morley N. Rituximab in the treatment of non-Hodgkin's lymphoma--a critical evaluation of randomized controlled trials. Expert opinion on biological therapy **2013**;13:803-11

42. Coiffier B, Thieblemont C, Van Den Neste E, Lepeu G, Plantier I, Castaigne S, *et al.* Long-term outcome of patients in the LNH-98.5 trial, the first randomized study comparing rituximab-CHOP to standard CHOP chemotherapy in DLBCL patients: a study by the Groupe d'Etudes des Lymphomes de l'Adulte. Blood **2010**;116:2040-5

43. Feugier P, Van Hoof A, Sebban C, Solal-Celigny P, Bouabdallah R, Ferme C, *et al.* Long-term results of the R-CHOP study in the treatment of elderly patients with diffuse large B-cell lymphoma: a study by the Groupe d'Etude des Lymphomes de l'Adulte. Journal of clinical oncology : official journal of the American Society of Clinical Oncology **2005**;23:4117-26

44. Pfreundschuh M, Trumper L, Osterborg A, Pettengell R, Trneny M, Imrie K, *et al.* CHOP-like chemotherapy plus rituximab versus CHOP-like chemotherapy alone in young patients with good-prognosis diffuse large-B-cell lymphoma: a randomised controlled trial by the MabThera International Trial (MInT) Group. The Lancet Oncology **2006**;7:379-91

45. Craxton A, Jiang A, Kurosaki T, Clark EA. Syk and Bruton's tyrosine kinase are required for B cell antigen receptor-mediated activation of the kinase Akt. The Journal of biological chemistry **1999**;274:30644-50

46. Petro JB, Rahman SM, Ballard DW, Khan WN. Bruton's tyrosine kinase is required for

activation of IkappaB kinase and nuclear factor kappaB in response to B cell receptor engagement. The Journal of experimental medicine **2000**;191:1745-54
47. Shaffer AL, Rosenwald A, Staudt LM. Lymphoid malignancies: the dark side of B-cell differentiation. Nature reviews Immunology **2002**;2:920-32
48. Wang ML, Rule S, Martin P, Goy A, Auer R, Kahl BS, *et al.* Targeting BTK with ibrutinib in relapsed or refractory mantle-cell lymphoma. The New England journal of medicine **2013**;369:507-16
49. Byrd JC, Furman RR, Coutre SE, Flinn IW, Burger JA, Blum KA, *et al.* Targeting BTK with ibrutinib in relapsed chronic lymphocytic leukemia. The New England journal of medicine **2013**;369:32-42
50. Treon SP, Xu L, Hunter Z. MYD88 Mutations and Response to Ibrutinib in Waldenstrom's Macroglobulinemia. The New England journal of medicine **2015**;373:584-6
51. Wilson WH, Young RM, Schmitz R, Yang Y, Pittaluga S, Wright G, *et al.* Targeting B cell receptor signaling with ibrutinib in diffuse large B cell lymphoma. **2015**;21:922-6
52. Tanaka H, Kaneko N, Sakagami H, Yamamoto H, Matsuya T, Hiramoto M, *et al.* Naquotinib exerts antitumor activity in activated B-cell-like diffuse large B-cell lymphoma. submitted to Molecular Cancer Therapeutics
53. Hur W, Velentza A, Kim S, Flatauer L, Jiang X, Valente D, *et al.* Clinical stage EGFR inhibitors irreversibly alkylate Bmx kinase. Bioorganic & medicinal chemistry letters **2008**;18:5916-9
54. Davis RE, Ngo VN, Lenz G, Tolar P, Young RM, Romesser PB, *et al.* Chronic active B-cell-receptor signalling in diffuse large B-cell lymphoma. Nature **2010**;463:88-92
55. Kozaki R, Vogler M, Walter HS. Responses to the Selective Bruton's Tyrosine Kinase (BTK) Inhibitor Tirabrutinib (ONO/GS-4059) in Diffuse Large B-cell Lymphoma Cell Lines. **2018**;10
56. Poulin P, Hop CE, Salphati L, Liederer BM. Correlation of tissue-plasma partition coefficients between normal tissues and subcutaneous xenografts of human tumor cell lines in mouse as a prediction tool of drug penetration in tumors. Journal of pharmaceutical sciences **2013**;102:1355-69
57. Yoshida M, Kobunai T, Aoyagi K, Saito H, Utsugi T, Wierzba K, *et al.* Specific distribution of TOP-53 to the lung and lung-localized tumor is determined by its interaction with phospholipids. Clinical cancer research : an official journal of the American Association for Cancer Research **2000**;6:4396-401